

A Coupled lattice Boltzmann-Multiparticle collision method for multi-resolution hydrodynamics

Andrea Montessori*

Istituto per le Applicazioni del Calcolo CNR, via dei Taurini 19, Rome, Italy

Adriano Tiribocchi

Center for Life Nano Science@La Sapienza, Istituto Italiano di Tecnologia, 00161 Roma, Italy

Marco Lauricella

Istituto per le Applicazioni del Calcolo CNR, via dei Taurini 19, Rome, Italy

Sauro Succi

Center for Life Nano Science@La Sapienza, Istituto Italiano di Tecnologia, 00161 Roma, Italy

Institute for Applied Computational Science, John A. Paulson School of Engineering and Applied Sciences, Harvard University, Cambridge, USA

Abstract

In this work we discuss the coupling of two mesoscopic approaches for fluid dynamics, namely the lattice Boltzmann method (LB) and the multiparticle collision dynamics (MPCD) [20] to design a new class of flexible and efficient multiscale schemes based on a dual representation of the fluid observables.

At variance with other commonly used multigrid methods, mostly oriented to high Reynolds and turbulent flows, the present approach is designed to capture the physics at the smallest scales whenever the lattice Boltzmann alone falls short of providing the correct physical information due to a lack of resolution, as it occurs for example in thin films between interacting bubbles or droplets in microfluidic crystals.

The coupling strategies employed to pass the hydrodynamic information

*a.montessori@iac.cnr.it

between the LB and the MPCD are detailed and the algorithm is tested against the steady isothermal Poiseuille flow problem for different coupling configurations.

Keywords:

1. Introduction

The development of efficient and accurate numerical models able to simulate fluids' behavior over a broad range of time and spatial scales still represents a grand challenge in computational physics, with a plethora of applications in science and engineering.

Notwithstanding the huge advancements and success obtained by computer simulations at the molecular and microscopic level (i.e. MD and DSMC approaches [7, 14, 1, 5]), direct simulation of complex flows at time and length scales of experimental relevance is still out of reach even for the most powerful supercomputers to date.

To this aim, multiscale and multiphysics approaches, able to reproduce the physical phenomena occurring at different length and time scales with less computational expenditure, are constantly in demand.

Many attempts have been deployed so far in order to tackle this problem and a number of concurrent hybrid approaches have been proposed to investigate a vast spectrum of physics problems, including soft matter and molecular fluids [2, 31], fluctuating hydrodynamics [33] as well as both dilute and dense hydrodynamics [14, 34, 11].

In these approaches, small portions of the domain are analysed at a finer scale level, whereas the remaining part is treated on a coarser and computationally less demanding level. Then, the transfer of information enabling the coupling and communication across the different regions takes place within a coupling region.

In this work we prospect the possibility of coupling two mesoscopic approaches for fluid dynamics, namely the lattice Boltzmann method (LB) [32, 28] and the multiparticle collision dynamics (MPCD) [20] to design a novel, flexible and efficient multigrid approach.

The lattice Boltzmann method (LB) is based on a minimal version of the Bathnagar-Gross-Krook equation [6], in which the computational molecules, namely a discrete set of probability distribution functions, propagate along the links of a cartesian lattice and collide on the nodes relaxing towards a

Maxwell-Boltzmann equilibrium while, in the the MPCD, the fluid is modeled by a collection of pointlike particles which freely stream and locally collide according to mass-momentum-energy conserving rules.

At variance with others commonly used multigrid methods, mostly oriented to high Reynolds and turbulent flows, the proposed approach is designed to capture the physics at the smallest scales, whenever the lattice Boltzmann alone falls short of providing the correct physical information due to a lack of resolution and of underlying physics (i.e. thermal fluctuations at the micro and nano scales), as occurs for example in thin films between interacting bubbles or droplets [26, 29] or in micro and nano-confined flows[27, 25].

In the following, we provide a brief summary of the two basic methods: the LB and the MPCD.

2. Methods

2.1. Lattice Boltzmann method

The lattice Boltzmann method [4] (LB) is based on a minimal version of the time-honored Bathnagar-Gross-Krook equation, in which the computational molecules, namely a discrete set of probability distribution functions, propagate along the links of a cartesian lattice and collide on the nodes relaxing towards a Maxwell-Boltzmann equilibrium. The LB equation reads as follows:

$$f_i(\vec{x} + \vec{c}_i \Delta t, t + \Delta t) = f_i(\vec{x}, t) + \frac{\Delta t}{\tau} [f_i^{eq}(\rho, \vec{u}) - f_i(\vec{x}, t)] \quad (1)$$

where $f_i(\vec{x}, t)$ is the discrete distribution function representing the probability of finding a particle at position \vec{x} and time t moving along the i -th lattice direction with a (discrete) velocity \vec{c}_i , i spanning over the lattice directions ($i=0, \dots, b$) [32, 28]. For the sake of simplicity, Δt is the lattice time step, usually set to unity.

The left hand side of the eq.1 is the streaming step, representing the free-flight of particles along the lattice directions, which hop from a site to neighboring ones.

The right hand side is the collision term which codes for the relaxation of the set of discrete distributions towards a local equilibrium f_i^{eq} , namely a truncated, low Mach number expansion of the Maxwell-Boltzmann distribution [32, 22].

In this work we employed a second-order isotropic nine speed two dimensional lattice ($b = 8$, $D2Q9$ lattice) equipped with a set of second-order expansion of the Maxwell-Boltzmann distribution function, which read as:

$$f_i^{eq} = w_i \rho \left[1 + \frac{\vec{c}_i \cdot \vec{u}}{c_s^2} + \frac{(\vec{c}_i \cdot \vec{u})^2}{2c_s^4} - \frac{\vec{u} \cdot \vec{u}}{2c_s^2} \right] \quad (2)$$

w_i being the weights of the discrete equilibrium distribution functions, $c_s^2 = \sum_i w_i c_i^2 = 1/3$ the squared lattice speed of sound, \vec{u} the macroscopic fluid velocity. Moreover, the relaxation parameter τ in equation 1 is linked to the fluid kinematic viscosity via the linear relation $\nu = c_s^2(\tau - \Delta t/2)$ [32].

The hydrodynamic moments located in \vec{x} at time t , up to the order supported by the lattice in use (density, linear momentum and momentum flux tensor for a second-order isotropic lattice [9]), can be obtained by the computation of local, linear weighted sums, namely, $\rho = \sum_i f_i$, $\rho \vec{u} = \sum_i f_i \vec{c}_i$ and $\Pi = \sum_i f_i (\vec{c}_i \vec{c}_i - c_s^2 \mathbf{I})$ being \mathbf{I} the identity matrix.

2.2. Multiparticle collision dynamics with Andersen Thermostat

An MPCD fluid is modeled by a large number of pointlike particles of mass m , typically of the order of $10^3 - 10^5$ in two dimensions [15, 18]. The evolution of the system during a simulation time step consists of the subsequent application of a streaming and a collision step. During the streaming step, the particles positions are updated via a forward Euler update rule:

$$\vec{r}_k(t + \delta t) = \vec{r}_k(t) + \vec{v}_k(t) \delta t \quad (3)$$

being \vec{r}_k the vector position and \vec{v}_k the velocity of the k -th particle and δt the value of the MPCD discrete time step.

The algorithm then proceeds with the collision step, following one of the several available approaches [30, 19, 3]. Among them, a possible choice for the collision is to perform stochastic rotations of the particle velocities relative to the center-of-mass momentum. In this case, the multiparticle collision model is usually referred to as Stochastic Rotation Dynamics (SRD) [24].

In the SRD, the domain is divided into cells of side a [15]. Multi-particle collisions are then performed within each cell, by rotating the velocity, \vec{v}_k , of each k -th particle with respect to the velocity of the cell center of mass, \vec{v}_{cm} , of all particles in the cell:

$$\vec{v}_k(t + \delta t) = \vec{v}_{cm}(t) + \mathcal{R}(\vec{v}_k(t) - \vec{v}_{cm}(t)) \quad (4)$$

In the above equation, \mathcal{R} is the rotation matrix, which rotates the particles of a given cell by an angle $\pm\alpha$ with uniform probability $[1/2, -1/2]$. Because mass, momentum, and energy are conserved locally the thermohydrodynamic equations of motion are captured in the continuum limit [12]. Moreover, since the energy is locally conserved and the volume is invariant under both streaming and collision, the system is described by a microcanonical distribution at thermodynamic equilibrium [15].

The kinematic viscosity of an SRD fluid can be derived using a kinetic approach [21] and, in two dimensions, reads as follows:

$$\nu = \frac{Nk_B T \delta t}{a^2} \left[\frac{N}{(N-1 + e^{-N})(1 - \cos(2\alpha))} \right] + \frac{m(1 - \cos(\alpha))}{12\delta t} (N-1 + e^{-N}) \quad (5)$$

being N is the average number of particles in a collision cell.

Nonetheless, a stochastic rotation of the particle velocities relative to the center-of-mass velocity is not the only possibility to perform multi-particle collisions. In particular, MPCD simulations can be performed directly in the canonical ensemble by employing an Andersen thermostat (MPCD-AT) [15, 30, 3].

In the MPCD-AT new relative velocities are generated during each computational step in each cell. Thus, the collision step in a MPCD-AT can be compactly written as [30]:

$$\vec{v}_k(t + \delta t) = \vec{v}_{cm}(t) + \delta \vec{v}_k^{ran} = \vec{v}_{cm}(t) + \vec{v}_k^{ran} - \frac{1}{N_c} \sum_{j \in \text{cell}} \vec{v}_j^{ran} \quad (6)$$

where \vec{v}_k^{ran} are random numbers drawn from a Gaussian distribution with variance $\sqrt{k_B T/m}$ and N_c is the actual number of particles in the collision cell, the sum running over all particles in a given cell.

The MPCD-AT is, at the same time, a collision procedure and a thermostat, thus no additional velocity rescaling is required in non-equilibrium simulations with viscous heating and, as mentioned above simulations are performed directly in the canonical ensemble [15].

In the MPCD with the Andersen Thermostat the kinematic viscosity takes the following form:

$$\nu = k_B T \Delta t \left[\frac{N}{N-1 + e^{-N}} - \frac{1}{2} \right] + \frac{a^2}{12\Delta t} \left[\frac{N-1 + e^{-N}}{N} \right] \quad (7)$$

In this work we opted for the MPCD with the Andersen thermostat since, although computationally more expensive than SRD, the relaxation times in the MPCD-AT generally decrease by increasing the number of particles per cell, while they increase in the SRD. Longer relaxation times imply larger number of time steps required for transport coefficients to reach their asymptotic values [20]. As a consequence the number of particles per cell commonly employed in a SRD simulation is usually confined to 5 – 20, restriction which does not apply to the MPCD-AT, where the relaxation times scale as $(\ln N)^{-1}$ [15].

2.3. Coupling Procedure

In this subsection we detail the coupling strategy employed to exchange the hydrodynamic information between the lattice Boltzmann and the multiparticle collision dynamics.

First, we start from the simplest coupling case, namely when $\Delta x_{LB} = \Delta x_{MPCD} = a$. In Figure 1, a sketch of the hybrid simulation domain is reported. The right region is the pure LB region (green area), while the left one represents the high resolution region (MPCD, light blue area) where the streaming-collision processes of the multiparticle collision dynamics are performed; the area in the middle is the buffer region (red), where the LB-MPCD coupling is performed via the generation of particles velocity from the LB values of the (local) linear momenta.

It is important to note that, in this work, we employ a one way coupling between the two approaches [16] (i.e., only LB to MPCD) since the LB runs on the entire domain, the information exchange between the two models is implemented in the coupling region while the MPCD run only in selected regions of the domain.

To be more specific, in all the simulations performed, the coupling region covers over only two lattice nodes, which has proved to be sufficient to obtain smooth transitions of the solutions between the grids.

The coupling algorithm proceeds as follows:

1) **LB step.** The LB model is run across the entire domain over a computational step (full streaming and collision process).

2) **Information exchange step.** In the coupling region the particles velocities are re-generated by drawing them from a normal distribution, generated via the Box-Muller algorithm [8]. It is worth noting that, periodic

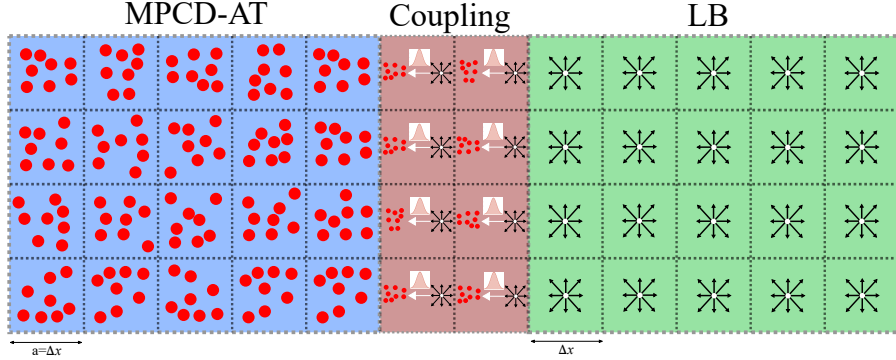


Figure 1: Representation of the hybrid domain. On the right region, the pure LB region (green area), and on the left, the high resolution (MPCD, light blue area) region where the streaming collision process of the multiparticle collision dynamics is performed; in the middle, the buffer region (red area) is drawn, where the $\text{LB} \rightarrow \text{MPCD}$ step is performed via the generation of particles velocity from the LB values of the (local) linear momenta.

boundary conditions are applied to each particle stepping into the LB region. It is worth noting that, periodic boundary conditions are applied to each particle which are in the process of exiting from the domain. In this way we avoid to inject new particles within the MPCD domain (the mass into the MPCD domain is exactly conserved), i.e. we perform simulations in an NVT (canonical) ensemble.

3) **MPCD step.** A full streaming and collision step of the MPCD-AT is performed within the MPCD region.

For the sake of clarity, A pseudo-code is reported in Algorithm 1

We then extended the hybrid MPCD-LB approach to run on multigrid (1 level of grid refinement) domains.

In particular, in the present implementation, the LB code runs on the coarse grid, which extends over the whole fluid domain, while the MPCD runs on a grid with half the spacing of the LB one (i.e. $a = 1/2$, see fig. 2 for a visual sketch of the multigrid hybrid domain).

The implementation follows the same procedure outlined in Algorithm 1 with an additional intermediate interpolation step between the LB and the MPCD steps, where the linear momentum is interpolated from the coarse to the fine grid (see Algorithm 2).

To this purpose we employed a simple bilinear interpolation.

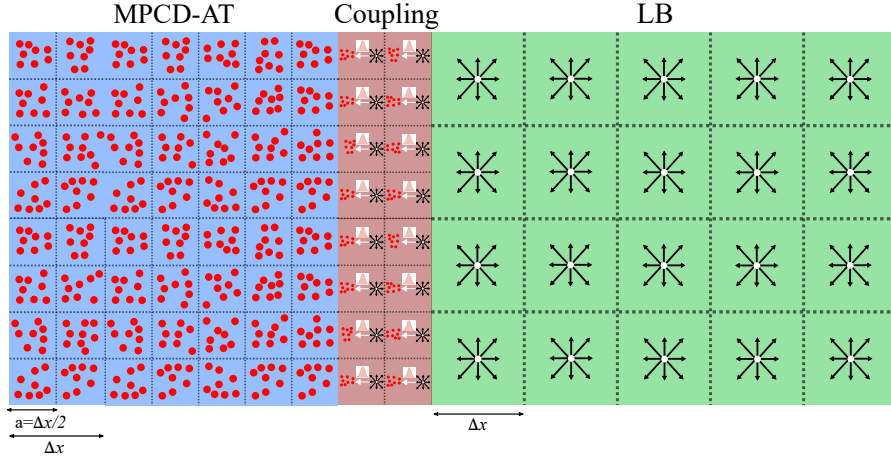


Figure 2: Representation of the hybrid multigrid (2 level) domain.

Algorithm 1 Coupling procedure : pseudo-code

- 1: **procedure** LB-MPCD COUPLING
 - 2: **LB step:**
 - 3:
 - 4: **call** LB collision
 - 5: **call** LB streaming
 - 6:
 - 7: **Information exchange step:**
 - 8: **for** particles \in coupling region draw $\vec{v}(\vec{x}, t)$ from $\frac{1}{\sqrt{2\pi k_B T}} e^{-\frac{(\vec{v}-u)^2}{2k_B T}}$
 - 9:
 - 10: **MPCD step**
 - 11: **call** MPCD streaming + boundary conditions
 - 12: **call** MPCD collision
-

Algorithm 2 Coupling procedure : pseudo-code

```
1: procedure LB-MPCD TWO LEVEL COUPLING
2:   LB step:
3:
4:   call LB collision
5:   call LB streaming
6:
7:   Bilinear interpolation step:
8:
9:   for  $i, j \in$  coupling region do  $\vec{u}_{coarse} \rightarrow \vec{u}_{fine}$ 
10:
11:  Information exchange step:
12:  for particles  $\in$  coupling region draw  $\vec{v}(\vec{x}, t)$  from  $\frac{1}{\sqrt{2\pi k_B T}} e^{-\frac{(\vec{v}-\vec{u})^2}{2k_B T}}$ 
13:
14:  MPCD step
15:  call MPCD streaming + boundary conditions
16:  call MPCD collision
```

Summarizing, in the present coupling approach, the information is transferred one-way only, from the LB to the MPCD domain. Consequently, the LB simulation is unaffected by the statistical thermal noise, generated within the particle domain, which is instead built-in within the MPCD method. It is also worth noting that, in [17] the equivalence between the velocity correlation function and the equipartition of kinetic energy has been demonstrated, thus confirming that the fluctuations in the MPCD fluid obeys the fluctuation dissipation theorem. As reported in Algorithms 1 and 2, after a full LB step, the information is sent to the MPCD domain via the generation of the particle velocities (sampled from a normal distribution) starting from the lattice Boltzmann linear momenta. In other words, this step works as a boundary condition for the MPCD. After the sampling within the buffer region, a streaming and collision step within the MPCD domain is performed.

As pointed out above, the coupling procedure is performed via the generation of the particle velocities in the overlapping region which are sampled from a Maxwell-Boltzmann distribution. This implies that, in the coupling region, the non-equilibrium part of the velocity distribution is set to zero. In the cases investigated in this work, this particular choice turned to be effec-

tive, not compromising the accuracy of the coupling procedure, as is shown in the following.

Nonetheless, the equilibrium coupling may become inaccurate in the presence of strong velocity gradients, where the non-equilibrium information of the velocity distribution cannot be ignored.

In these cases, different approaches, for example the sampling of the particle velocities from an Enskog distribution [13, 10], must be employed.

3. Results

The hybrid approach was tested against the steady isothermal Poiseuille flow problem.

The flow is driven by a constant body force which acts as a pressure gradient along the channel.

Along the flow direction we imposed periodic boundary conditions while, on the walls, no-slip conditions are employed.

No slip conditions have been implemented with a second-order scheme (half-way bounceback [22]) within the LB environment while, in the MPCD, we used the method proposed by Lamura et al. in [23].

Three cases have been considered:

1) Standalone LB and MPCD-AT simulations. This first set up was used to calibrate and test the MPCD and to compare the two models in terms of computational time.

2) Coupled LB-MPCD using the same spatial resolution with the coupling region positioned at the center of the channel.

3) Coupled LB-MPCD with near-wall grid refinement(1 level of grid refinement).

The simulation parameters for these three sets of simulations are reported in Table 1, for the reader's convenience.

3.1. Standalone LB and MPCD-AT

First, we run two separate sets of simulations to test the LB and MPCD-AT.

As stated above we run the classical Poiseuille flow benchmark between two parallel plates. The fluid domain is discretized with a 30×30 nodes grid.

As to the boundary conditions, as stated above, in both simulations we applied no slip conditions on the upper and lower walls and periodic boundary conditions along the flow direction.

Table 1: Simulations parameters: $nx \times ny$ grid points, Δx_{LB} lattice unit, a bin size, $\nu_{LB}(\tau)$ LB viscosity (LB relaxation time), ν_{MPCD} MPCD viscosity, $(k_B T)$ MPCD thermal energy, N MPCD particles, N_s MPCD sampling interval, g gravity (Body Force)

	$nx \times ny$	Δx_{LB}	a	ν_{LB} (τ)	ν_{MPCD} ($k_B T$)	N	N_s	g
1)	30×30	1	1	0.167(1.0)	0.167(~ 0.17)	$60 \div 600$	100	$5 \cdot 10^{-4}$
2)	30×30	1	1	0.167(1.0)	0.167(~ 0.17)	1000	100	$5 \cdot 10^{-4}$
3)	30×30	1	1/2	0.167(1.0)	0.167(~ 0.3)	1000	100	$5 \cdot 10^{-4}$

The kinematic viscosity (ν) and the body force (g), acting as a pressure gradient in the direction of the flow, have been set at the same values in both sets of simulations, so as to perform a one-to-one comparison between the two models.

All others relevant simulation parameters are reported in Table 1 for the sake of clarity.

First we compared the steady state solutions of the MPCD and LB simulations against the analytical solution for the two-dimensional Poiseuille velocity profile.

The results, reported in figure 3, confirm the accuracy of both the MPCD-AT and the LB, which are able to reproduce the Poiseuille flow with a very good degree of accuracy.

As per the MPCD-AT, we performed four different simulations by varying the number of particle per cell between $N = 60$ and $N = 600$.

In each case, the velocity profiles are averaged over $N_s = 100$.

In fact, a time averaging procedure is necessary to reduce the statistical noise associated with the particle nature of the MPCD.

Furthermore, as one can see in figure 3(a-d), the statistical noise decreases for increasing values of N .

Indeed, as is well known, the standard deviation on the fluid velocity can be expressed (at equilibrium) as:

$$\sigma_u = \sqrt{\frac{k_B T}{N}} \frac{1}{\sqrt{N_s}} \quad (8)$$

where N_s is the number of independent statistical samples.

From this relation the statistical error due to the evaluation of the velocity

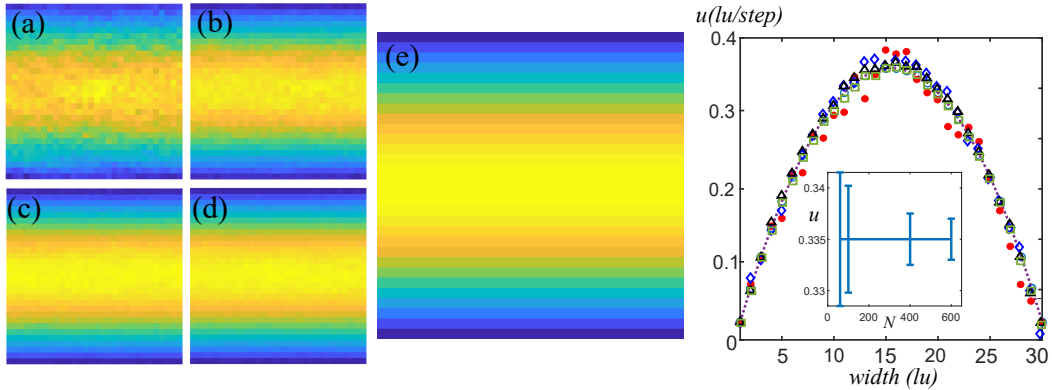


Figure 3: (a-d) Poiseuille flow velocity field. MPCD simulations with 60,100,400 and 600 particles per cell. (e) Poiseuille flow velocity field for the LB model. (f) Steady state velocity profiles (dotted line(analytic solution), red circles(MPCD,60 particles per cell), blue diamonds(MPCD,100 particles per cell), black triangles(MPCD,400 particles per cell), green squares(MPCD,600 particles per cell) and hollow light blue circles(LB solution)). Inset: standard deviation of the velocity in the centre of the channel as a function of N .

can be estimated as follows:

$$E_u = \frac{\sigma_u}{\bar{U}} \quad (9)$$

which is a rough estimate of the statistical error associated to the flow field at hand. In the equation above, \bar{U} is the average value of the flow velocity.

As a check, we computed the standard deviations of the MPCD simulations reported in fig. 3 (a-d), which range between $0.07 \div 0.0028$ for $N = 60 \div 600$, thus in close agreement with the formula reported above. In the inset of fig.3(e), we reported the standard deviation of the velocity in the centre of the channel as a function of N .

3.1.1. Computational performance

It is now interesting to compare the computational times associated with the LB and MPCD simulations.

To start, we note that a particle update (streaming and collision) takes $\sim 0.1\mu s/particle/step$ which is comparable to the time needed to update a lattice unit in a single component LB code $10 MLUPS$ (i.e. Mega Lattice Updates per Second), which is a typical performance of a serial implementation of a single phase, LB code [22].

It is clear that, in the case of the MPCD model, the running times scale roughly linearly with the total number of particles within the domain and, in our simulations, vary between $0.01s/step \div 0.1s/step$ with the particle densities ranging between $60 \div 600$ particles per bin.

With these numbers in mind, an efficient parallelization able to exploit the computational capabilities of the latest supercomputers is needed in order to make the coupling approach amenable to large scale simulations.

It is finally worth noting that, the performance data reported above refer to a serial implementation of the code, run on a Intel Xeon Platinum 8176 CPU based on the Skylake microarchitecture. The code was compiled by Intel Fortran Compiler version 18.0.2 with the recent AVX-512 instruction set supported on Skylake architectures.

3.2. Coupled LB-MPCD-AT: center line coupling

We then applied the coupling procedure presented above to the same test case.

The main results are shown in figure 4.

As reported above, the LB run over a grid covering whole the fluid domain while the MPCD grid is restricted only to the lower half of the fluid domain.

The information is transferred at the center line of the domain, where the coupling procedure is applied.

As stated above, the depth of the coupling zone, is two lattice units and is denoted by the region included within the dashed line in figure 4(a-d).

We run four separate cases for different values of the density of MPCD particles per cell, which ranges between $60 \div 1000$ ((a) to (d)).

The grids share the same spatial discretization and the same kinematic viscosity, $\nu = 0.167 lu^2/step$.

As one can see, the flow fields smoothly connect in the coupling region even for the smallest value of the particle density.

It is evident that, by increasing the number of particles the statistical error associated to the flow field decreases accordingly, this being evidenced in panel (e) of the same figure which reports the LB and the MPCD velocity profiles which smoothly overlap for $N = 1000$.

In the same plot, a comparison between the continuous (MPCD) and discrete (LB) velocity distribution functions at the steady state is reported (inset of figure 4(e)).

The inset displays the time-space averaged velocity distribution. It is interesting to note that while the MPCD velocity distribution ($2d$ field) keeps

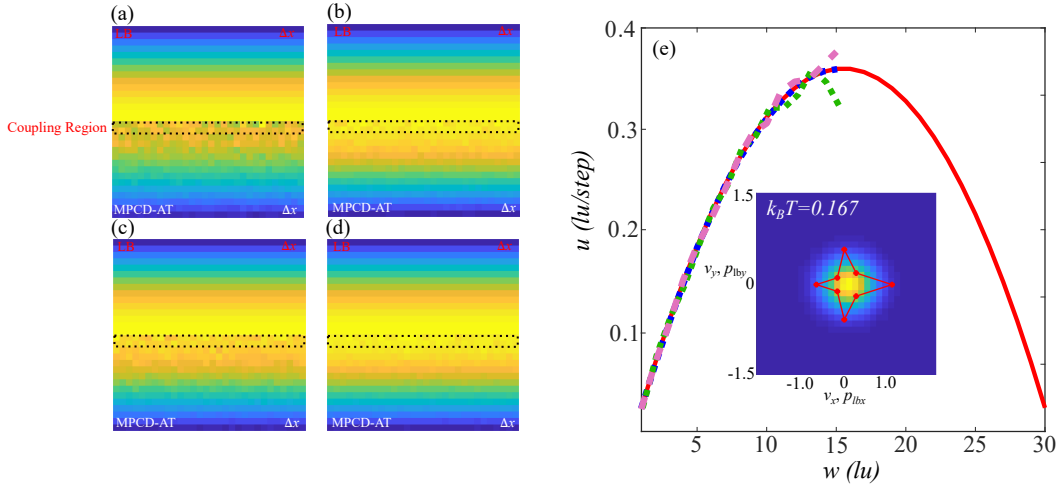


Figure 4: (a-d) Hybrid approach, Poiseuille flow velocity field. The Coupling region is denoted by dotted region. The cell density of particles was varied between $60 \div 1000$ ((a) 60, (b) 150, (c) 300, (d) 1000). (e) Plot of the velocity profiles, LB solution (solid line) MPCD (dashed lines) for different values of N . Inset: time-space averaged velocity distribution, comparison between LB(spider plot) and MPCD ($2d$ histogram).

its typical (shifted) Maxwell-Boltzmann shape the LB distributions (spider plot) more skewed, its skewness increasing for larger values of the mean channel velocity (i.e. as the average Mach number increases). This departure from the Maxwell-Boltzmann behavior is due to the fact that the set of lattice distributions is not allowed to shift (i.e., the largest probability is always associated to the rest particle), as instead occurs in the continuous case, but it occurs via a positive bias in the co-flowing distributions.

For this reason, the larger the non-equilibrium (represented in this case by the large values of the mean channel velocity) the larger the skewness of the discrete set of distributions.

3.3. Coupled LB-MPCD-AT: near-wall, two level coupling

We then tested the capability of the hybrid approach to handle multi-level grids correctly.

To this purpose, we run two separate simulations:

1) the LB and the MPCD share the same grid discretization. The LB runs on a 40×60 nodes grid and is coupled to the MPCD near the wall which runs on a 40×14 bins grid.

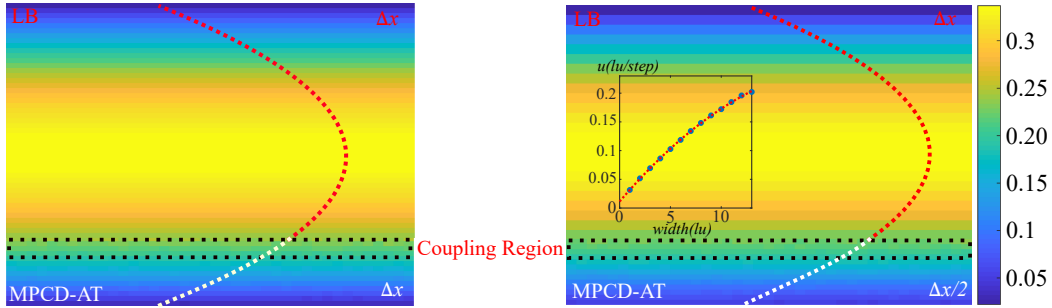


Figure 5: (a) Coupled LB-MPCD approach with the same grid discretization (fine grid simulation). (b) Hybrid approach with grid refinement at the wall. Inset : Comparison between the analytical solution of the Poiseuille flow near the wall and the MPCD solution.

2) the LB runs on a 20×30 nodes grid (halved with respect to the previous case), and is coupled near the wall to the MPCD which runs on 39×13 grid with a halved discretization ($a = 1/2$) with respect to the LB grid.

The first case is employed as a reference case to test the ability of the coupling procedure to correctly reproduce the Navier-Stokes solution and to handle multigrid domains.

Also in this case, the overlapping zone extends to two lattice units and $N = 1000$ particles/cell.

The main results are reported in figure 5.

As one can see, the velocity profiles smoothly reconnect in the overlapping region and the number of time samples and particles per cell are sufficient to suppress the statistical oscillations inherent to the MPCD algorithm.

This is also quantitatively confirmed by the comparison between the analytical solution near the wall and the MPCD averaged velocity profile which perfectly overlap, as shown in the inset of fig. 5, thus further corroborating the accuracy of the hybrid approach.

4. Conclusions

In this work we have developed a multi-level procedure to couple a lattice Boltzmann approach concurrently with a multiparticle collision approach, the goal being to build a hybrid multigrid Navier-Stokes solver.

At variance with other commonly employed multigrid methods for high Reynolds and turbulent flows, the proposed approach is designed to capture the physics at the smallest scales whenever the lattice Boltzmann alone falls short of providing the correct physical information due to a lack of resolution and of underlying physics (i.e. thermal fluctuations).

The hybrid model has been applied to the classical Poiseuille flow across two parallel plates and several cases have been investigated, namely 1) standalone LB and MPCD-AT simulations, 2) coupled LB-MPCD with the coupling region positioned at the center of the channel, 3) Coupled LB-MPCD with near-wall grid refinement (1 level of grid refinement).

Further developments of the proposed model (currently ongoing) will aim at the simulation of complex fluid phenomena occurring in nanoconfined systems and also within thin films between fluid interfaces where both resolution and thermal fluctuations are required to forecast the correct physics.

Acknowledgements

A. M., M. L., A. T. and S. S. acknowledge funding from the European Research Council under the European 196 Unions Horizon 2020 Framework Programme (No. FP/2014-2020) ERC Grant Agreement No.739964 (COP-MAT).

References

- [1] Berni J Alder and Thomas Everett Wainwright. Studies in molecular dynamics. i. general method. *The Journal of Chemical Physics*, 31(2):459–466, 1959.
- [2] Uliana Alekseeva, Roland G Winkler, and Godehard Sutmann. Hydrodynamics in adaptive resolution particle simulations: Multiparticle collision dynamics. *Journal of computational physics*, 314:14–34, 2016.
- [3] E Allahyarov and G Gompper. Mesoscopic solvent simulations: Multiparticle-collision dynamics of three-dimensional flows. *Physical Review E*, 66(3):036702, 2002.
- [4] R. Benzi, S. Succi, and M Vergassola. The lattice boltzmann equation: theory and applications. *Phys. Rep.*, 222(3):145–197, 1992.

- [5] Herman JC Berendsen, David van der Spoel, and Rudi van Drunen. Gromacs: a message-passing parallel molecular dynamics implementation. *Computer physics communications*, 91(1-3):43–56, 1995.
- [6] Prabhu Lal Bhatnagar, Eugene P Gross, and Max Krook. A model for collision processes in gases. i. small amplitude processes in charged and neutral one-component systems. *Physical review*, 94(3):511, 1954.
- [7] GA Bird. Monte carlo simulation of gas flows. *Annual Review of Fluid Mechanics*, 10(1):11–31, 1978.
- [8] George EP Box. A note on the generation of random normal deviates. *Ann. Math. Stat.*, 29:610–611, 1958.
- [9] Hudong Chen, Isaac Goldhirsch, and Steven A Orszag. Discrete rotational symmetry, moment isotropy, and higher order lattice boltzmann models. *Journal of Scientific Computing*, 34(1):87–112, 2008.
- [10] G. Di Staso, H. J. H. Clercx, S. Succi, and F. Toschi. Dsmc-lbm mapping scheme for rarefied and non-rarefied gas flows. *J. Comp. Sci.*, 17:357–369, 2016.
- [11] G Di Staso, HJH Clercx, S Succi, and F Toschi. Lattice boltzmann accelerated direct simulation monte carlo for dilute gas flow simulations. *Philosophical Transactions of the Royal Society A: Mathematical, Physical and Engineering Sciences*, 374(2080):20160226, 2016.
- [12] Uriel Frisch, Brosl Hasslacher, and Yves Pomeau. Lattice-gas automata for the navier-stokes equation. *Physical review letters*, 56(14):1505, 1986.
- [13] Alejandro L Garcia and Berni J Alder. Generation of the chapman-enskog distribution. *Journal of computational physics*, 140(1):66–70, 1998.
- [14] Alejandro L Garcia, John B Bell, William Y Crutchfield, and Berni J Alder. Adaptive mesh and algorithm refinement using direct simulation monte carlo. *Journal of computational Physics*, 154(1):134–155, 1999.
- [15] G Gompper, T Ihle, DM Kroll, and RG Winkler. Multi-particle collision dynamics: A particle-based mesoscale simulation approach to the hydrodynamics of complex fluids. *Advances in polymer science*, 221(PreJuSER-3284):1–87, 2009.

- [16] D Hash and H Hassan. A decoupled dsmc/navier-stokes analysis of a transitional flow experiment. In *34th aerospace sciences meeting and exhibit*, page 353, 1996.
- [17] Chien-Cheng Huang, Gerhard Gompper, and Roland G Winkler. Hydrodynamic correlations in multiparticle collision dynamics fluids. *Physical Review E*, 86(5):056711, 2012.
- [18] T Ihle and DM Kroll. Stochastic rotation dynamics: A galilean-invariant mesoscopic model for fluid flow. *Physical Review E*, 63(2):020201, 2001.
- [19] Thomas Ihle, E Tüzel, and Daniel M Kroll. Consistent particle-based algorithm with a non-ideal equation of state. *EPL (Europhysics Letters)*, 73(5):664, 2006.
- [20] Raymond Kapral. Multiparticle collision dynamics: Simulation of complex systems on mesoscales. *Advances in Chemical Physics*, 140:89, 2008.
- [21] N Kikuchi, CM Pooley, JF Ryder, and JM Yeomans. Transport coefficients of a mesoscopic fluid dynamics model. *The Journal of chemical physics*, 119(12):6388–6395, 2003.
- [22] Timm Krüger, Halim Kusumaatmaja, Alexandr Kuzmin, Orest Shardt, Goncalo Silva, and Erlend Magnus Viggen. The lattice boltzmann method. *Springer International Publishing*, 10:978–3, 2017.
- [23] Antonio Lamura, Gerhard Gompper, Thomas Ihle, and DM Kroll. Multi-particle collision dynamics: Flow around a circular and a square cylinder. *EPL (Europhysics Letters)*, 56(3):319, 2001.
- [24] Anatoly Malevanets and Raymond Kapral. Mesoscopic model for solvent dynamics. *The Journal of chemical physics*, 110(17):8605–8613, 1999.
- [25] Alireza Mohammadzadeh, Ehsan Roohi, and Hamid Niazmand. A parallel dsmc investigation of monatomic/diatomic gas flows in a micro/nano cavity. *Numerical Heat Transfer, Part A: Applications*, 63(4):305–325, 2013.
- [26] A Montessori, M Lauricella, N Tirelli, and S Succi. Mesoscale modelling of near-contact interactions for complex flowing interfaces. *Journal of Fluid Mechanics*, 872:327–347, 2019.

- [27] A. Montessori, P. Prestininzi, M. La Rocca, and S. Succi. Lattice boltzmann approach for complex nonequilibrium flows. *Phys. Rev. E*, 92(4):043308, 2015.
- [28] Andrea Montessori and Giacomo Falcucci. *Lattice Boltzmann modeling of complex flows for engineering applications*. Morgan & Claypool Publishers, 2018.
- [29] Andrea Montessori, Marco Lauricella, Adriano Tiribocchi, and Sauro Succi. Modeling pattern formation in soft flowing crystals. *Physical Review Fluids*, 4(7):072201, 2019.
- [30] Hiroshi Noguchi, Norio Kikuchi, and Gerhard Gompper. Particle-based mesoscale hydrodynamic techniques. *EPL (Europhysics Letters)*, 78(1):10005, 2007.
- [31] Raffaello Potestio, Sebastian Fritsch, Pep Espanol, Rafael Delgado-Buscalioni, Kurt Kremer, Ralf Everaers, and Davide Donadio. Hamiltonian adaptive resolution simulation for molecular liquids. *Physical review letters*, 110(10):108301, 2013.
- [32] S. Succi. *The Lattice Boltzmann Equation: For Complex States of Flowing Matter*. Oxford University Press, 2018.
- [33] Sumesh P Thampi, Ignacio Pagonabarraga, and Ronjoy Adhikari. Lattice-boltzmann-langevin simulations of binary mixtures. *Physical Review E*, 84(4):046709, 2011.
- [34] Thomas Werder, Jens H Walther, and Petros Koumoutsakos. Hybrid atomistic–continuum method for the simulation of dense fluid flows. *Journal of Computational Physics*, 205(1):373–390, 2005.